Environmental Science Nano

PAPER

View Article Online
View Journal | View Issue

Cite this: *Environ. Sci.: Nano*, 2015, **2**, 615

Gene expression as an indicator of the molecular response and toxicity in the bacterium *Shewanella oneidensis* and the water flea *Daphnia magna* exposed to functionalized gold nanoparticles†

T. A. Qiu,‡[a] J. S. Bozich,‡[b] S. E. Lohse,[c] A. M. Vartanian,[c] L. M. Jacob,[c] B. M. Meyer,[a] I. L. Gunsolus,[a] N. J. Niemuth,[b] C. J. Murphy,[c] C. L. Haynes[a] and R. D. Klaper*[b]

Nanoparticle (NP) physiochemical properties have been shown to be important determinants of NP interactions with biological systems. Due to both nanomaterial diversity and environmental complexity, a mechanistic understanding of how physiochemical properties affect NP/organism interactions will greatly aid in the accurate assessment and prediction of current and emerging NP-induced environmental impacts. Herein, we investigated key biological apical endpoints, such as viability, growth, and reproduction and the expression of genes associated with related molecular pathways in response to exposure to gold nanoparticles (AuNPs) functionalized with either positively charged ligands, polyallyamine hydrochloride, or negatively charged ligands, mercaptopropionic acid, in two model organisms, the bacterium *Shewanella oneidensis* MR-1 and the water flea *Daphnia magna*. By linking changes in molecular pathways to apical endpoints, potential biomarkers for functionalized AuNP impacts were identified in both organisms. Specifically, *act* was identified as a potential biomarker in *D. magna* and 16S as a potential biomarker in *S. oneidensis*. We also revealed that changes in molecular pathways induced by ligand–NP combination were strongly dependent upon the type of ligand on the NP surface, and the effects from their respective ligands alone might predict these effects for the ligand–NP combination, but only in some cases. Lastly, we revealed that it is possible to identify similar pathways provoked upon NP exposure across organisms. This study shows that molecular pathways will help elucidate mechanisms for NP toxicity that are predictive of adverse environmental outcomes.

Received 7th March 2015,
Accepted 2nd August 2015

DOI: 10.1039/c5en00037h

rsc.li/es-nano

Nano impact

Based on the great diversity of organisms in the environment and possible engineered nanomaterials, fundamental understanding of nanoparticle-biological interactions will be critical for accurate assessment and prediction of nanoparticle environmental impacts. Herein, we investigated key biological apical endpoints and molecular pathways in response to functionalized Au nanoparticles in two environmentally relevant model organisms, the bacterium *Shewanella oneidensis* and the water flea *Daphnia magna*. We identified some specific molecular responses that may serve as potential biomarkers for nanoparticle impacts, revealed that changes in apical endpoints and molecular pathways in both organisms strongly depend on ligand-nanoparticle combination, and uncovered shared pathways provoked upon nanoparticle exposure. This study facilitates a better understanding of nanoparticle-organism interaction mechanisms, building toward prediction of meaningful environmental outcomes.

Introduction

Engineered nanoparticles (NPs) are being produced to enhance a wide range of societally beneficial applications, from energy storage capacities and material durability to medical therapeutics and water treatment devices.[1–3] These applications are possible because of the novel physiochemical properties NPs display, such as high surface area and reactivity as well as distinct surface chemistries, compositions and size distributions. It is, however, these same size-dependent physiochemical properties that may influence

[a] *Department of Chemistry, University of Minnesota, 207 Pleasant St SE, Minneapolis, MN 55455, USA*
[b] *School of Freshwater Sciences, University of Wisconsin Milwaukee, 600 E. Greenfield Ave, Milwaukee, WI 53204, USA. E-mail: rklaper@uwm.edu; Fax: +414 382 1705; Tel: +414 382 1713*
[c] *Department of Chemistry, University of Illinois at Urbana-Champaign, 600 S. Mathews Ave, Urbana, IL 61801, USA*

† Electronic supplementary information (ESI) available. See DOI: 10.1039/c5en00037h

‡ These two authors contributed equally to this work.

their biocompatibility.[4–8] For example, size, shape and core composition have been thought to mediate receptor–ligand binding rates, cellular phagocytosis, exocytosis and cytotoxicity.[9–12] Other studies suggest that NP surface charge is the main determinant of biological interactions, with positively charged particles being more toxic than negatively or neutrally charged particles.[13–18]

These classifications of critical features that determine biological impact all focus on the NPs themselves. The differences in response across organisms or cell types are less often considered despite the fact that toxicological evaluations of the biological impacts caused by engineered NPs have revealed a wide range in responses across cell types or organisms considered.[19–23] For example, Sohaebuddin *et al.* (2010)[24] demonstrated that cell type determines the extent of response to nanomaterials with different compositions and sizes. In another study using ZnO NPs, the EC_{50} differed by orders of magnitude for *V. fischeri*, *D. magna* and *T. platyurus*.[25] Variation across cell systems and organisms makes it difficult to develop a common understanding of the properties of nanomaterials that may determine toxicity. Even for well-studied chemicals, such as pesticides, models that use general acute endpoint data to predict impacts often inaccurately estimate concentrations that cause effects across similar chemicals and rarely are applicable across organisms.[26,27] These studies have shown that a more mechanistic understanding of the impacts of chemicals at sublethal doses provides a more accurate description of impacts and better data for modeling these effects across species. The goal of this project is to achieve a more mechanistic understanding of NP/organism interactions to facilitate efficient prediction of the impact nanotechnology will have on environmental health. Linking specific molecular mechanisms that are impacted by NPs across organisms to apical endpoints will not only greatly aid in assessing the potential environmental impact of these materials but is also crucial to informing NP design for safe and sustainable development of nanotechnologies.

Currently, the major proposed molecular mechanism for NP toxicity is oxidative stress.[4,28–31] However, the exposures that produce oxidative stress in many studies are well above what is estimated to be the current or future environmental concentrations; long-term low dose exposures are the more likely scenario.[32,33] In addition, the molecular mechanisms responsible for coping with oxidative stress are triggered upon exposure to a wide range of chemical species[34,35] and are a natural biological response that does not necessarily lead to an adverse outcome.[36] The focus on oxidative stress and lethal dose exposures makes it difficult to uncover other mechanisms that may have a greater predictive power for the environmental impact of NPs. Sublethal concentration-based exposures allow the cell to have a more natural perturbation by the contaminant that triggers subtle, but potentially specific, molecular responses.[37,38] It is these more realistic exposure scenarios that will uncover more mechanism-based information to predict meaningful impacts across species.

Molecular biomarkers provide a sensitive indicator of the response of an organism to stressors such as exposure to a toxicant in addition to providing information on the mechanisms that are impacted by exposure.[37,38] Mechanistic information that can be tied to larger impacts on reproduction for example enhances the possibility of predicting negative outcomes where standardized toxicological tests, although valuable, have limited ability to accurately predict the impact of emerging contaminants. Overreliance on these methods has led to risk assessment failures.[39] Developing such candidate biomarkers for NP toxicity will greatly aid in the rapid assessment and impact prediction for current and emerging nanomaterials across a wide range of organisms. Previously developed biomarkers, for example, vitellogenin, have been used for the successful determination of adverse outcomes of some classes of endocrine disruptors and their impacts on vertebrate reproduction.[40–42] Metallothioneins are used to detect metal ion exposure, and they are expressed in response to a wide range of metal-based contaminants associated with environmental pollution.[43] Heat shock proteins, indicative of proteotoxic stressors, indicate subtlethal cellular damage and respond in a dose-dependent manner to environmental stressors.[44] Biomarkers that provide mechanistic insight into nanoparticle-organism interactions, especially if they apply to effects seen across species, would provide a way to group nanomaterials by their molecular level effects. Furthermore, they may indicate both nonspecific and specific modes of action as well as underlying mechanisms for toxicity of NPs with particular physiochemical properties.

In this study, we examined several candidate biomarkers in two model species, the bacterium *Shewanella oneidensis* and the invertebrate *Daphnia magna*, that are associated with pathways of importance in these two species and determined how their expression related to the biological impacts of exposure to gold NPs (AuNPs) with positively or negatively charged surfaces. *Shewanella oneidensis* (MR-1) is an environmentally beneficial Gram-negative bacterium with a unique metal-reducing capability to respire heavy metals; *S. oneidensis* plays an important role in the cycling of metal elements in the ecosystem as well as the bioremediation of toxic elements.[45] *Daphnia magna* is a designated toxicology and toxicogenomics model organism by multiple agencies (OECD, NIH and EPA) and is an environmentally relevant freshwater invertebrate that composes an integral part of freshwater food webs.[46] AuNPs were chosen as a model NP in this study due to the chemical inertness of the gold core and our ability to readily control size,[47] shape[48] and surface functionalization.[49] Two ligands were used for AuNP functionalization, positively charged polyallylamine hydrochloride (PAH) and negatively charged mercaptopropionic acid (MPA).

We explored genes in various molecular pathways in our two model organisms. Pairs of genes selected from each organism were to represent pathways encoding for similar cellular functions in the two organisms, including oxidative

stress, xenobiotic detoxification, protein folding, cellular electron transport, and cellular maintenance. In addition, genes in pathways related to reproduction in *D. magna* and to cell division, DNA repair and extracytoplasmic stress in *S. oneidensis* were also investigated. The goal was to determine: 1) how the exposure to NPs with differing surface properties impacted each organism and how this differed from their respective ligand controls; 2) if gene expression for these pathways were an indication of impacts seen in each organism; 3) if exposure duration altered effects and gene expression measurements and if acute measurements of gene expression would provide an indication of chronic impacts; and 4) if gene expression for similar pathways across organisms would provide biomarkers that were predictive across species. The NPs used in this study were quantitatively and qualitatively characterized prior to and after exposure to assay media to aid us in understanding how alterations in NP physical properties may impact molecular pathways. Overall, this work aims to link molecular pathways and apical endpoints to NP characteristics in two distinct environmentally relevant organisms.

Methods

Functionalized AuNP synthesis and characterization

All materials were used as received, unless otherwise noted. Gold tetrachloroaurate trihydrate ($HAuCl_4{\cdot}3H_2O$), sodium borohydride ($NaBH_4$), trisodium citrate, 3-mercaptopropionic acid (MPA) and polyallylamine hydrochloride (PAH; M_w 15 000 g mol^{-1}) were obtained from Sigma Aldrich. Ultrapure deionized water was prepared using a Barnstead NANOPURE water filtration system. PALL Minimate tangential flow filtration capsules for AuNP purification with 50 kDa pore size was obtained from VWR. Transmission electron microscopy grids were obtained from PELCO (SiO on copper mesh).

The 4.7 (±1.5) nm-diameter PAH–AuNPs were prepared by polyelectrolyte wrapping of ~4 nm-diameter citrate-coated AuNPs. The (4.3 ± 1.3) nm-diameter MPA–AuNPs were prepared by direct synthesis. After synthesis, measuring and counting using TEM images determined size distributions. Detailed descriptions of the AuNP syntheses are given below.

PAH–AuNPs (4.7 ± 1.5 nm). As a first step in synthesis of PAH–AuNPs, citrate AuNPs were synthesized using previously reported procedures.[47] In an *aqua regia*-cleaned round-bottomed flask, 5.0 mL of aqueous gold tetrachloroaurate hydrate ($HAuCl_4{\cdot}3H_2O$, 10.0 mM) was combined with 1.5 mL of aqueous 0.1 M sodium citrate and diluted to a final volume of 400 mL with ultrapure deionized water. The reaction mixture was stirred vigorously for 10 min. An aqueous solution of ice-cold 10.0 mM sodium borohydride (30.0 mL) was then added to the reaction mixture, while stirring continued. Following borohydride addition, the solution rapidly changed color to a deep brown and then red-orange over the course of the first 10 minutes of stirring. The resulting AuNP solution was then stirred for a further 3.0 hours. The crude 4 nm Cit–AuNPs were then concentrated using a diafiltration apparatus, prior to polyelectrolyte wrapping.[50] Cit–AuNPs were then wrapped with polyallylamine hydrochloride (PAH) to prepare 4 nm PAH–AuNPs, as previously described.[51] Briefly, the concentrated Cit–AuNP solution was dispersed in 20.0 mL of a 1.0 mM aqueous sodium chloride solution to give a final AuNP concentration of approximately 20.0 nM. To each 20.0 mL of polyelectrolyte wrapping solution, 500 μL of 15 000 M_w PAH (10.0 mg mL^{-1}) dissolved in 1.0 mM NaCl was then added. The wrapping solution was briefly mixed at vortex briefly and left to stand for 16 h. The PAH–AuNPs were subsequently purified by centrifugation and washing (55 min at 18 894 rcf), in ultrapure deionized water. The purified PAH–AuNPs were then concentrated in a diafiltration membrane.[50]

MPA–AuNPs (4.3 ± 1.3 nm). MPA-stabilized AuNPs were prepared by direct synthesis with sodium borohydride according to previously reported methods.[52] Briefly, a 500 mL aqueous solution of $HAuCl_4$ (1.5 mM) and MPA (3.0 mM) was prepared using ultrapure deionized water in an *aqua regia*-cleaned round-bottomed flask. The pH of the growth solution was adjusted to approximately 8.5 by the addition of dilute aqueous sodium hydroxide and stirred at vortex for 10 min. 10.0 mL of a 0.1 M aqueous sodium borohydride solution was then added to the reaction mixture. The combined solutions rapidly changed color to a deep orange-brown, and the reaction mixture was stirred for a further 3 hours. The thiol-stabilized AuNPs were then concentrated and purified by diafiltration (40.0 volume equivalents of ultrapure deionized water in a 50 kDa membrane).

AuNP characterization and analysis

Synthesized functionalized AuNPs were characterized in Milli-Q water, bacteria growth medium, and *Daphnia* medium using various analytical techniques, including TEM for absolute sizes (JEOL 2100 Cryo TEM), dynamic light scattering for hydrodynamic diameter (Brookhaven ZetaPALS), zeta-potential for surface charge (Brookhaven ZetaPALS), and UV-vis localized surface plasmon resonance (LSPR) spectroscopy for particle concentration and aggregation (Mikropack DH-2000 UV-vis-NIR spectrometer).

Free ligand suspensions

Free ligands, MPA and PAH (M_w 15 000 g mol^{-1}), were obtained from Sigma Aldrich. MPA and PAH ligands are readily soluble in water and do not require a co-solvent for dispersion. The ligands were dissolved into Milli-Q water at a maximum concentration of 50 mg L^{-1} and diluted accordingly for free ligand toxicity control experiments.

Shewanella oneidensis MR-1 cultivation and cell oxygen uptake assay

***S. oneidensis* MR-1 cultivation.** *S. oneidensis* MR-1 was obtained from Professor Jeffery Gralnick, University of Minnesota Department of Microbiology and was stored at −80 °C before use. Bacteria were inoculated onto a LB broth agar plate and incubated at 30 °C for 24 hours or until visible colonies formed. A minimal medium consisting of salts and

buffering agent was used in this study. 0.68 g NaCl, 0.3 g KCl, 0.285 g $MgCl_2 \cdot 6H_2O$, 0.3975 g Na_2SO_4, 0.15 g NH_4Cl, and 2.383 g HEPES (4-(2-hydroxyethyl) piperazine-1-ethanesulfonic acid) were dissolved in 1 liter of Milli-Q water. After autoclaving and cooling down, 0.0125 g Na_2HPO_4 and 0.0056 g $CaCl_2$ were added per liter. Right before use, 1.86 mL sodium DL-lactate syrup (60% w/w, Sigma-Aldrich) was mixed with the minimal medium to make 100 mL of the final growth medium containing 129 mM sodium DL-lactate. Lactate was used as an additional carbon source to promote bacterial growth. Colonies formed on agar plates were inoculated into the minimal medium with lactate in sterile culture tubes and grown in a 32 °C orbital shaker at 300 rpm until OD_{600} ~ 0.25, the maximal optical density that *Shewanella oneidensis* MR-1 can reach in the minimal medium with lactate.

Monitoring *S. oneidensis* oxygen uptake. The oxygen uptake of the bacteria population over time was monitored using a PF-8000 aerobic/anaerobic respirometer system (Respirometer Systems and Applications, LLC). Bacteria were grown in minimal medium with lactate until it reached OD_{600} ~ 0.25 and diluted 1 : 10 into the growth medium supplied with NP/ligands in reaction vessels that were kept in a 32 °C water bath. Exposures of PAH–NPs were conducted at 30, 100, and 5000 μg L^{-1}, and exposures of PAH ligand were 30, 100, 300, 600, 1000, 2000 and 5000 μg L^{-1}. In all subsequent experiments and comparisons, a ten-fold mass concentration of PAH free ligand and an equivalent mass concentration of MPA free ligand were used as ligand controls, which was calculated to be an overestimate of possible total free ligand present in the suspension (see ESI†).[53] A tube filled with 1 mL 30% (w/w) KOH solution was inserted into each reaction vessel to absorb carbon dioxide generated from cell respiration. The consumption of oxygen was compensated by continuous oxygen injection to keep the pressure constant in the headspace of the reaction vessels. Oxygen uptake was recorded every 10 minutes automatically for 24–48 hours by the instrument. The first derivative of oxygen uptake was plotted to identify the maximal oxygen uptake rate and the time of that maximum. To represent each oxygen uptake trace with a single value, the ratio of maximal oxygen uptake rate to the time when it reached maximal rate was calculated following the equation below:

$$\text{Ratio} = \frac{\text{Maximal rate } (\text{mg h}^{-1})}{\text{Time to reach maximal rate } (\text{h})}$$

The ratio was then normalized to the average of control groups and represented as a percentage, where 100% indicates no inhibition of cell oxygen uptake.

Daphnia magna cultivation and biological assays

***D. magna* cultivation.** Populations used in this experiment were cultivated at the UW-Milwaukee School of Freshwater Sciences in the R. Klaper laboratory. *Daphnia* neonates used for the gene expression assays were collected from populations maintained in moderately hard reconstituted water (MHRW) incubated at 20 °C on a 16 : 8 light/dark cycle as designated by EPA protocols.[54] *Daphnia* breeding populations were held at a concentration of 14 adult *Daphnia* per 1 L of media in glass beakers and were discarded once adults reached 28 days old. *Daphnia* were fed 50 mL freshwater algae (*Pseudokirchneriella subcapitata*) at an algal density of 400 000 algal cells per mL and 15 mL of dissolved alfalfa (*Medicago sativa*). Alfalfa stock was prepared by suspending 405 mg of Alfalfa in 50 mL Milli-Q water after 15 minutes of stirring and 5 minutes of centrifugation at 3829 RCF.

***D. magna* acute assay.** Acute survival assays were carried out in a 48 h static exposure. All exposures used 5 *Daphnia* neonates (24–48 hours old) per 100 mL of MHRW (control), NPs, or free ligands suspended in MHRW, bringing the total volume to 100 mL. A minimum of three replicates were carried out for each treatment, and survival was determined as percentage alive at 48 h. Exposures were carried out to determine sublethal concentrations of NPs and free ligands. Concentrations tested for NPs and free ligands are: 1, 5, 10, 50, 100 μg L^{-1} for PAH–AuNPs and PAH free ligand and 1, 5, 10 and 25 mg L^{-1} for MPA–AuNPs and MPA free ligand.

***D. magna* chronic assay.** *Daphnia* chronic exposures used 5 *Daphnia* neonates (24–48 hours old) exposed to NPs or ligands for 21 days in a static renewal exposure, and triplicate assays were performed for each condition. A total of 5 neonates were placed in 94 mL of MHRW (control) or NPs/ligands where full media change out occurred three times per week. In chronic exposures, daphnids are supplemented with 4 mL of algae (*Selenastrum capricornitum*) and 2 mL of alfalfa (*Medicago sativa*) at each media exchange to bring the total volume to 100 mL. Concentrations tested in the chronic assay were: 1 and 5 μg L^{-1} for PAH–AuNPs and PAH free ligand and 5 and 25 mg L^{-1} for MPA–AuNPs and MPA free ligand. Reproduction and mortality were measured at each media exchange, and body size was recorded at the end of the exposure.

Reproductive exposures adhered to the mortality and reproduction guidelines designated by the OECD (OECD guidelines 1998). Daphnids were kept at a concentration of 5 daphnids per 100 mL, and results were normalized to controls (*i.e.* daphnia exposed to only MHRW) to account for changes in reproduction and body size as these replicate exposures took place over a period of several months.

Gene expression exposures and RNA preservation

Gene expression exposures were performed in parallel with bacterial oxygen uptake and *D. magna* survival and reproduction assays.

***S. oneidensis*.** Colonies from agar plates were inoculated in minimal medium supplied with 129 mM lactate until the

bacterial suspension reached OD_{600} ~ 0.25. The bacterial suspension was adjusted to OD_{600} ~ 0.2 before AuNPs were added. The sublethal dosages, 30 μg L^{-1} of PAH–AuNPs and 300 μg L^{-1} of PAH ligand, and 5 mg L^{-1} of MPA–AuNPs and MPA ligands, were primarily used for gene expression studies; in addition, a 100 μg L^{-1} dose of PAH–AuNPs was used to investigate two biomarker candidates, in order to provide further evidence to link molecular pathways to inhibition of bacterial oxygen uptake. After NPs/ligands were added, the bacterial suspension was incubated on a 32 °C orbital shaker at 300 rpm for 1 hour or 6 hours. Cells were harvested by centrifuging at 1500 × g for 10 minutes, and then the pellets were sufficiently re-suspended into either 200 μL (PAH–AuNP/ligand) or 1 mL (MPA–AuNP/ligand) of RNAzol®RT (Molecular Research Center, Inc.) for cell lysis and RNA preservation.

D. magna. *Daphnia* neonates (24–48 hours old) were exposed to NPs and free ligands in an acute exposure lasting 24 hours. All exposures used 10 neonates per 100 mL of MHRW (control) or NPs or free ligands suspended in MHRW (treatment) bringing the total volume to 100 mL. Exposures were carried out at sublethal concentrations of NPs/free ligands between 5–1000 μg L^{-1} depending on the NP/free ligand being considered. Sublethal concentrations for acute exposures were chosen based on previous study (Bozich *et al.* 2014). Greater than three replicates were carried out for each treatment and concentration tested. At the end of the exposure duration, daphnids were collected and put in a 1.5 mL RNase-free eppendorf tube corresponding to their replicate number. Excess liquid was removed, and daphnids were immediately flash frozen in liquid nitrogen and stored at −80 °C to wait further processing. For *D. magna* chronic exposures, exposures were carried out at sublethal concentrations of NPs/free ligands between 5–5000 μg L^{-1}, and daphnids were collected at the end of the 21 day exposure period and preserved using the same method as the acute exposure samples. The RNA from all samples was extracted using TRIzol® for cell lysis and RNA preservation.

RNA extraction, reverse transcription and real-time quantitative PCR

A Direct-zol™ RNA MiniPrep kit (Zymo Research) was used for total RNA isolation and purification by spin columns. The manufacturer's recommended protocol was followed using a centrifugation speed of 12 000 × *g* with an on-column DNase I treatment at 30 °C for 15 minutes. RNA was finally eluted from the column at 16 000 × *g* for 1 minute. Total RNA was characterized using a Thermo Scientific NanoDrop 8000 and an Agilent 2100 Bioanalyzer for quality control.

Total RNA was reverse transcribed into cDNA following the manufacturer's protocols. Briefly, 100 ng of total RNA were incubated in the presence of either random primers (Promega) for *S. oneidensis* or oligo$(dT)_{15}$ primer (Promega) for *D. magna* at 65 °C for 5 minutes. After cooling on ice for 1 minute, the SuperScript III reverse transcriptase, DTT, and RNaseOUT™ recombinant ribonuclease inhibitor (Life Technologies) were added into the mixture followed by incubation at 25 °C for 5 minutes (this step was only for random primers), 50 °C for 60 minutes, and 70 °C for 15 minutes for primer extension. Once synthesized, cDNA were stored at −20 °C.

Target genes were chosen for both *S. oneidensis* and *D. magna*. Four pairs of genes in similar pathways related to stress response in the two organisms were selected, including *gst* (*S. oneidensis*)/*gst* (*D. magna*, same order for the following pairs) in xenobiotic detoxification, *nqrF*/*nadh* for electron transport, *katB*/*cat* for oxidative stress attenuation, and *ibpA*/*hsp70* for heat shock response. To link to apical endpoints, the *vtg* gene for *D. magna* reproduction and *ftsK* for bacterial cell division were also examined. Genes for actin (*act*) in *D. magna* and for 16S ribosomal RNA (16S) and RNA polymerase (*rpoA*) in *S. oneidensis* were monitored to consider NP/ligand impacts on basic organism machinery. In addition, stress response genes including *pspB* for extracytoplasmic stress, *sodB* for oxidative stress, and *radA* for DNA repair were also examined in *S. oneidensis*. Table 1 shows a full list of genes along with their corresponding functions.

Primers for real-time quantitative PCR were designed by the PrimerQuest Tool (Integrated DNA Technologies). Two sets of primers were designed for each gene, and the one with efficiency closest to 1 was chosen to be the primer for subsequent real-time PCR. Table 1 includes a full list of primers used in this study.

Real-time quantitative PCR (qPCR) was performed on a StepOnePlus™ Real-Time PCR System (Life Technologies) using SYBR Green as the fluorescent intercalating dye (iTaq™ Universal SYBR® Green Supermix, Bio-Rad). For each qPCR reaction, cDNA and primers were mixed with the fluorescence dye following the manufacturer's protocol. Starting with an initial 10 min denaturation at 95 °C, real-time PCR repeated 40 cycles of amplification, each of which was 15 s at 95 °C followed by 30 s at 60 °C. Fluorescence of SYBR Green was detected at the end of each cycle. All qPCR experiments were done in technical duplicates.

NORMA-Gene analysis of qPCR data

Real-time quantitative PCR data were processed by the Miner[55] program and NORMA-Gene algorithm.[56] Miner applies an objective analysis scheme to obtain the dynamic fluorescence threshold (R), threshold cycle number (C_t), and efficiency (E) for each qPCR reaction, instead of using the same threshold for all reactions. Data for the normalized reporter signal (R_n) *versus* cycle number were extracted from amplification data exported from the StepOnePlus™ software as the input to the Miner program to obtain R, C_t, and E values for each reaction. R_0, the initial fluorescent reporter signal, was calculated based on the equation below:

$$R_0 = R \times (1 + E)^{-C_t}$$

Due to the change in housekeeping genes throughout experiments, NORMA-Gene, a qPCR normalization method based

Table 1 Target genes, corresponding functions, and their primers for qPCR

Shewanella oneidensis MR-1

Target gene	Forward primer (5′–3′)	Reverse primer (5′–3′)	Function	Accession number
Glutathione *S*-transferase (*gst*)	GCA AAG CAT TCC AGC AAT TT	GAC CTT CTT GCG TTT TGA GC	Xenobiotic detoxification	NP_720213.1
Na-translocating NADH-quinone reductase subunit F (*nqrF*)	CGC TTA CTC GAT GGC TAA CTA C	GCA AGG CAG CGT CAA ATT AC	Mitochondrial electron transport NADH to ubiquinone	NP_716734.1
Double-stranded DNA translocase (*ftsK*)	TAC GAG TCG TGT TGC GAT AAA	AAG GGC TGA CAC TGG AAT AAA	Cell division	NP_717901.1
Catalase HPII (*katB*)	GGC ATT GAT CCT GAT TCT TCT C	TCC AAC GAG GGA AGT TAC CA	Catalase activity; response to oxidative stress	NP_716697.1
16 kDa heat shock protein A (*ibpA*)	GCA ACT CAG GTT ATC CTC CAT AC	CGC TAC TGA TCT CAA GCT CTT C	Response to heat; chaperone activity	NP_717873.1
16S ribosomal RNA (16S)	TCA AGT CAT CAT GGC CCT TAC	TAC GAC GAG CTT TGT GAG ATT AG	Component of prokaryotic ribosomes	NR_074798.1
RNA polymerase alpha subunit (*rpoA*)	TCG CAT CCT ATT GTC GTC TAT G	CTT CTT GTA CGC CTT CCT TAC T	DNA-directed RNA polymerase activity	NP_715896.1
ATP-dependent protease (*radA*)	TTC GGC AAT TTT CCT CTC C	ACA CCA CCA TGA CCA AGG AT	DNA repair	NP_716849.1
Phage shock protein B (*pspB*)	TTG ATT GCG AAA GCC GAT A	ATC AAG AAT CGC CTC TAA GGT TT	Extracytoplasmic stress	NP_717416.1
Fe/Mn superoxide dismutase (*sodB*)	GCA ATG TTC GCC CTG ACT AC	CCT GCG AAG TTT TGG TTC AC	Removal of superoxide radicals	NP_718453.1

Daphnia magna

Target gene	Forward primer (5′–3′)	Reverse primer (5′–3′)	Function	
Glutathione *S*-transferase (*gst*)	CAA CGC GTA TGG CAA AGA TG	CTA GAC CGA AAC GGT GGT AAA	Xenobiotic detoxification	AF448500.1
Dehydrogenase (*nadh*)	GCA GGA AAC AAT AAG GCA AAC C	GGT GGC ACA GAC CAT TTC TTA	Mitochondrial electron transport and energy production	DQ340845.1
Vitellogenin (*vtg*)	CTG TTC CTC GCT CTG TCT TG	CCA GAG AAG GAA GCG TTG TAG	Reproduction, sexual maturation and general stress	AB252737.1
Catalase (*cat*)	CAG GAT CAT CGG CAG TTA GTT	CTG AAG GCA AAC CTG TCT ACT	Oxidative stress attenuation	GQ389639.1
Heat shock protein 70 (*hsp70*)	CCT TAG TCA TGG CTC GTT CTC	TCA AGC GGA ACA CCA CTA TC	Response to heat; protein folding	EU514494.1
β-Actin (*act*)	CCA CAC TGT CCC CAT TTA TGA A	CGC GAC CAG CCA AAT CC	Cytoskeleton production and cell maintenance	AJ292554.1

on target gene data, was applied to normalize the gene expression data and reduce the variation among replicates rather than using a single housekeeping gene.[56] Using this technique, the geometric means of R_0 values of technical duplicates were calculated as the average and were put into the NORMA-Gene workbook generously provided by Dr. Yuya Hayashi. Normalized R_0 values, which were the output of NORMA-Gene algorithm, were then further normalized to control groups by dividing the normalized R_0 of treated groups by the geometric mean of normalized R_0 values of control groups to obtain the relative fold change.

Statistical analysis

The normalized ratios from oxygen uptake traces were further subjected to statistical analysis. No normality and outliers were considered within this data set due to the limited sample size ($N < 5$). The two-tailed student's *t*-test was performed on treated samples *versus* their respective control group with $\alpha = 0.05$. GraphPad Prism (GraphPad Software, Inc.) was used for statistical analysis.

Data from *Daphnia* acute studies failed to meet the assumptions of normality. Therefore, the effects of NP and free ligand exposures on *Daphnia* survival, were compared to controls using the nonparametric Mann–Whitney *U* test for two-independent samples ($N > 3$). Impacts on daphnid reproduction and body size were assessed using one-way ANOVA with Tukey's multiple comparison tests after normality and variance homogeneity were determined ($N > 3$). One round of statistically determined outliers was removed, and treatments were deemed significantly different than controls at probability value <0.05. SPSS (IBM 2013) was used to interpret data.

The relative fold change values of *S. oneidensis* gene expression were $\log_2$-transformed followed by the combination of control groups. Outliers were identified and excluded from the data set (ROUT algorithm, Q = 1.0%, Prism GraphPad), and *post hoc* Tukey's tests after ANOVA were performed to determine statistical significance among different treatments at one time point and one gene of interest. For the 16S and *sodB* genes upon 100 μg L^{-1} PAH–AuNP exposure, as there was only one treatment, an unpaired *t*-test was used instead of ANOVA. Again, normality was not tested due

to the limited sample size ($N < 6$). GraphPad Prism was used to perform statistical analysis.

The relative gene expression data from *Daphnia* short-term and long-term gene exposures were normalized to controls and $\log_2$ transformed to fit a normal distribution. Outliers were removed prior to statistical analysis. Significant differences in relative expression were determined using one-way ANOVA with Tukey's multiple comparison tests after normality and variance homogeneity were determined ($p < 0.05$) ($N > 3$). SPSS (IBM 2013) was used to interpret data.

Results

Nanoparticle characterization

TEM analysis of absolute size showed that the two AuNPs had very similar core size, while the hydrodynamic diameter of PAH–AuNPs in water was larger than MPA–AuNPs, possibly due to the polyelectrolyte wrapping (Table 2). It was notable that MPA–AuNPs showed an increased hydrodynamic diameter and a peak shift in UV-vis extinction upon resuspension in growth medium, indicating the aggregation of MPA–AuNPs, though the MPA–AuNPs still retained a negative surface charge in the growth medium (Table 2). The aggregation may result from elevated ionic strength in the growth medium or the pH change from slightly acidic Milli-Q water (pH ~ 6.3) to neutral growth medium (pH ~ 7.2). This aggregation might lead to altered NP toxicity, as previous studies have revealed.[19,57] Similar behavior was not observed for PAH–AuNPs, indicating more stability of PAH–AuNPs than MPA-AuNPs in growth medium (Table 2).

Shewanella oneidensis oxygen uptake

PAH–AuNPs significantly affected bacterial oxygen uptake at 100 μg L^{-1} (unpaired *t*-test, $t = 9.895$, df = 5, $p < 0.05$) while its corresponding free ligand control, 1 mg L^{-1} of PAH free ligand elicited similar inhibition compared to control groups (unpaired *t*-test, $t = 4.222$, df = 6, $p < 0.05$) (Fig. 1(c)). A concentration of 30 μg L^{-1} of PAH–AuNPs was chosen as the sublethal dose as this concentration produced no inhibition; this NP dose was paired with the 10-fold dose, 300 μg L^{-1}, as the corresponding PAH free ligand control. MPA–AuNPs did not inhibit bacterial oxygen uptake at the highest dose tested (5 mg L^{-1}), while the

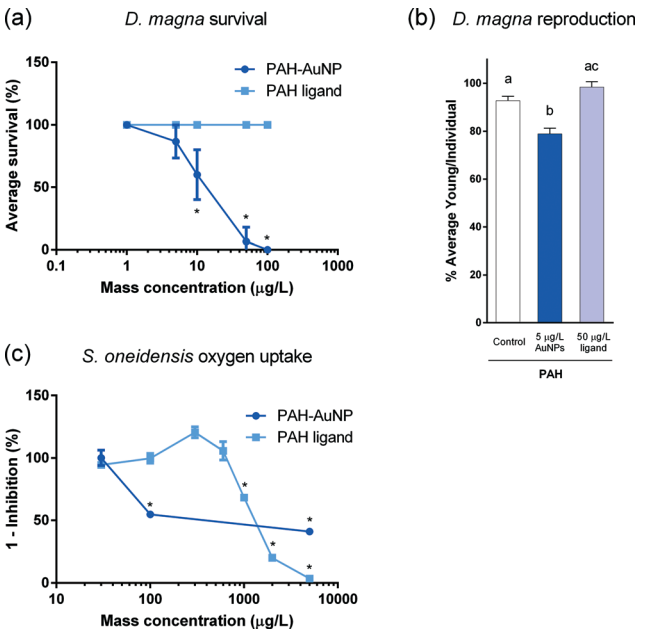

Fig. 1 Impact of PAH–AuNPs and PAH ligand on (a) *D. magna* survival (%), (b) *D. magna* reproduction and (c) *S. oneidensis* oxygen uptake. Error bars represent standard error of the mean. Stars indicate significant difference compared to corresponding control groups (*S. oneidensis*, unpaired *t*-test, $\alpha = 0.05$, $n \geq 2$; *D. magna*, unpaired *t*-test, $\alpha = 0.05$, $n \geq 3$). Different letter designations in (b) indicate significant difference between groups (Tukey's test, $\alpha = 0.05$).

respective 5 mg L^{-1} of MPA free ligand demonstrated oxygen uptake inhibition ($t = 9.713$, df = 2, $p < 0.05$) (Fig. S2†).

As the oxygen uptake reflects bacterial population growth, the doubling time of bacterial growth at the exponential phase was calculated based on oxygen uptake traces (see ESI†). Results showed that *S. oneidensis* had an average doubling time between 2 and 3 hours in the growth medium used in this study; thus, 1 hour was chosen as a time point for short-term exposure and 6 hour for long-term exposure in the subsequent gene expression studies.

S. oneidensis gene expression response

At the sublethal exposure dosages, differential expression levels of ten genes in *S. oneidensis* were observed at both 1

Table 2 Nanoparticle characterization

	PAH–AuNPs		MPA–AuNPs	
	S. oneidensis media	*D. magna* media	*S. oneidensis* media	*D. magna* media
LSPR λ_{max} (nm) (in H_2O)[a]	528		515	
LSPR λ_{max} (nm) (in medium)	530	530	555	575
d_{core} (nm)*	4.7 ± 1.5 ($N \geq 250$)		4.3 ± 1.3 nm ($N = 501$)	
D_h (nm) (in H_2O)	200.2 ± 3.5		126.4 ± 3.7	
D_h (nm) (in medium)	159.5 ± 0.6	79.43 ± 1.9	339.6 ± 21.9	364 ± 34.2
ζ-Potential (mV) (in H_2O)	+68.5 ± 1.6		−17.3 ± 0.6	
ζ-Potential (mV) (in medium)	+24.57 ± 5.6	+10.5 ± 4.8	−24.28 ± 3.2	−29.8 ± 1.3

*Based on TEM analysis. See Fig. S1 for TEM images. [a] Localized surface plasmon resonance (LSPR) wavelength of maximum peak value (λ_{max}). Errors are represented by standard deviations.

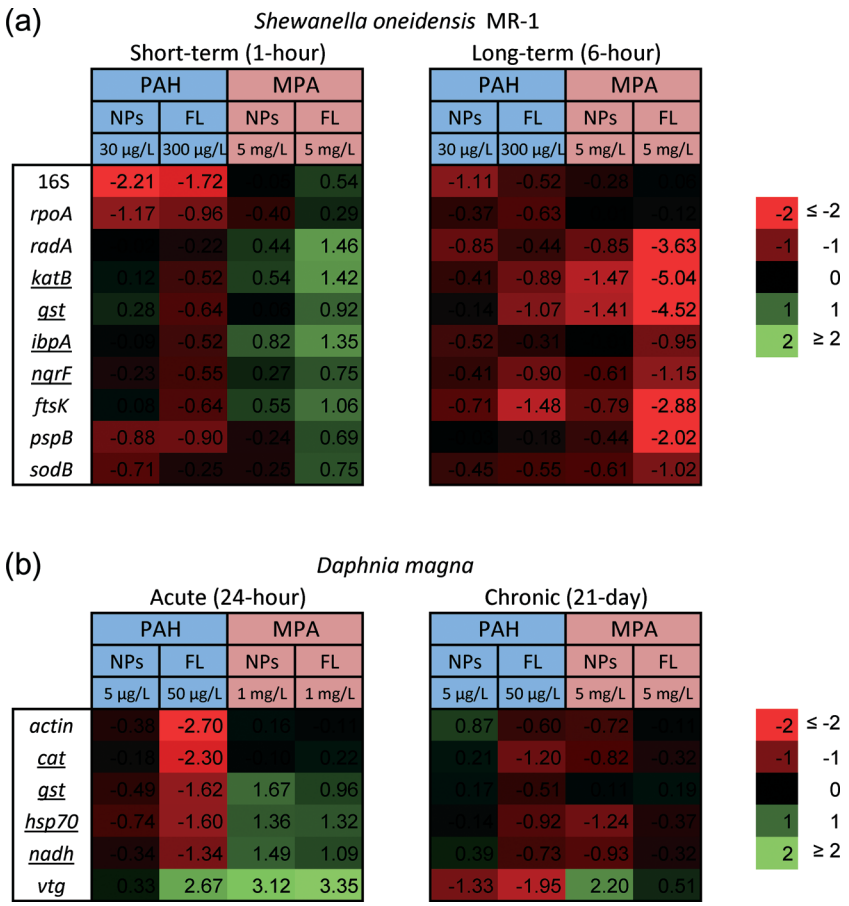

Fig. 2 Heat map of (a) *S. oneidensis* and (b) *D. magna* gene expression response. Sublethal dosages of AuNPs and their respective ligand control were used in the gene expression study, as shown in the figure. Genes encoding for similar cellular functions in two model organisms are underlined.

hour and 6 hour time points when comparing treatment and control. The general pattern of gene expression is summarized in the heat map (Fig. 2(a)).

In all cases, the differences in gene expression appear to be dominated by ligand rather than NP exposure. All changes in gene expression induced by ligand–NP combination were accompanied by the changes in their respective free ligand control, including 16S (PAH, $F = 18.33$, df = 22, $p < 0.0001$), *rpoA* (PAH, $F = 8.177$, df = 31, $p = 0.0001$), *pspB* (PAH, $F = 8.198$, df = 22, $p < 0.0003$), and *ibpA* (MPA, $F = 36.92$, df = 22, $p < 0.0001$) at 1 hour exposure (Fig. 3(a)), and *sodB* (PAH and MPA, $F = 10.06$, df = 22, $p < 0.0001$) at 6 hour exposure (Fig. 3(b)). Exceptions are two NP-specific effects that were observed in *sodB* (PAH, $F = 7.543$, df = 22, $p < 0.05$) at 1 hour exposure and 16S (PAH, $F = 3.238$, df = 22, $p < 0.05$) at 6 hour exposure, where the free ligand control did not elicit similar effects as NPs when compared to control. For these two genes, *S. oneidensis* was exposed to a higher dosage (100 μg L^{-1}) of PAH–AuNPs to explore the link to inhibition of oxygen uptake (Fig. 4). The 16S gene expression decreased upon 100 μg L^{-1} PAH–AuNP exposure at 6 hour exposure (unpaired *t*-test, $t = 38.67$, df = 7, $p < 0.0001$), while *sodB* gene expression did not show a significant difference compared to the control group at 1 hour exposure.

The difference in ligand–NP combination appears to be important in determining the differential gene expression pattern at 1 hour exposure, as only down-regulation was observed in PAH–AuNP exposure but only up-regulation was observed in MPA–AuNP exposure (Fig. 2(a)). However, upon 6 hour exposure, the ligand–NP combination did not determine the gene expression pattern, as only down-regulation was observed for all treatments, regardless of the type of ligand (Fig. 2(a)).

Time frame is also an important factor in terms of gene expression response, as differential gene expression responses were observed at different time points. In response to PAH–AuNP/ligand exposure, effects that were observed in the *rpoA* and *pspB* genes at 1 hour exposure diminished by the 6 hour exposure timepoint. More interestingly, for MPA–AuNP/ligand exposure, the expression level compared to control at the 6 hour exposure appeared to be opposite of the response in the 1 hour exposure, especially for MPA ligand exposure.

Daphnia magna acute toxicity

NP surface functionalization played an important role in acute toxicity in the form of daphnid survival, with positively charged PAH–AuNPs being orders of magnitude more toxic

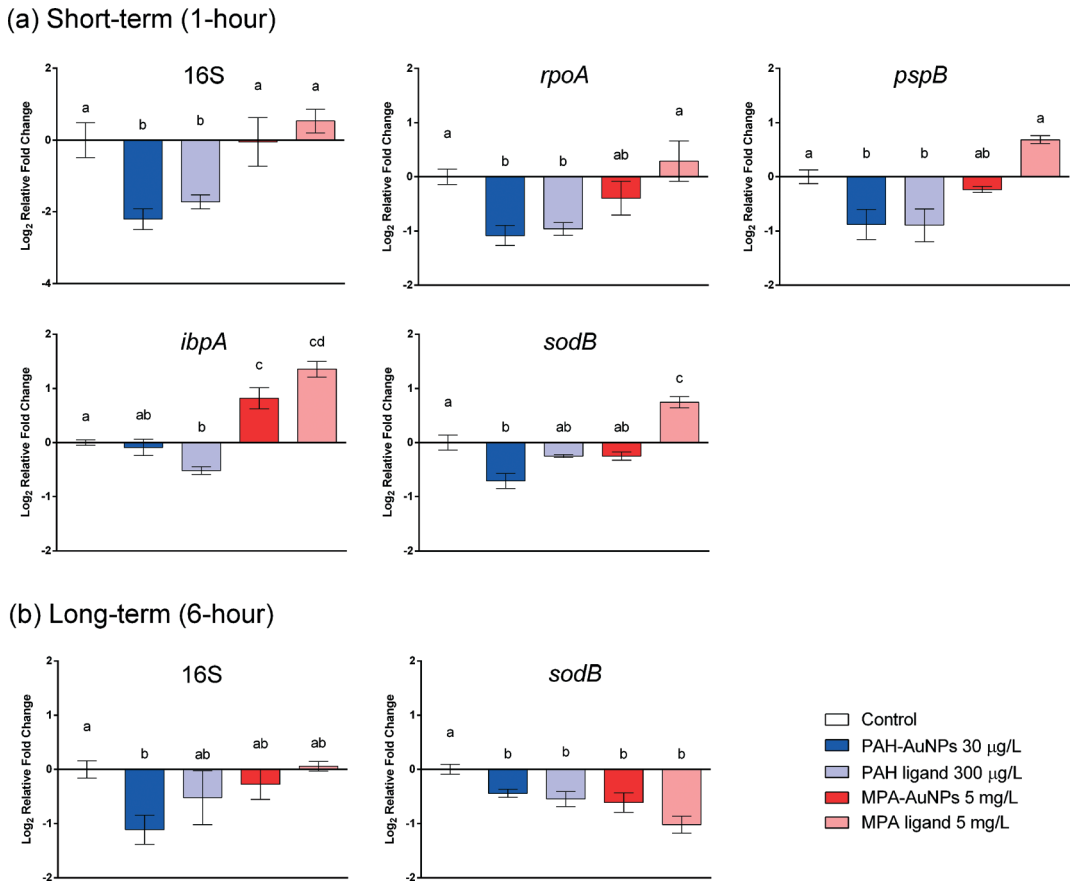

Fig. 3 Selected gene responses in *S. oneidensis* upon AuNP/ligand exposure. Error bars show standard error of the mean (PAH–AuNP, n = 5; PAH ligand, n = 4; MPA–AuNP/ligand, n = 3). All figures follow the same legend, and the first bar in every figure indicates control group. Different letter designations between different groups indicate significant difference (Tukey's test, α = 0.05).

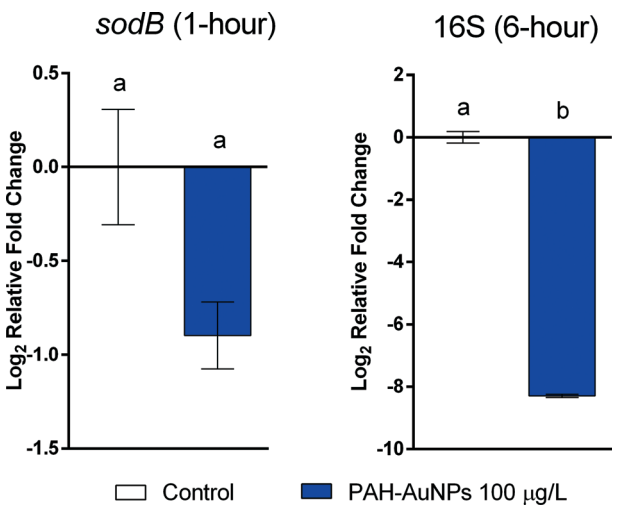

Fig. 4 In *S. oneidensis*, 16S gene expression decreased upon 100 μg L^{-1} PAH–AuNP exposure at long-term exposure (6 hour), while *sodB* gene expression did not show significant difference compared to control group. Error bars show standard error of the mean ($n \geq 4$). Both figures follow the same legend. Different letter designations indicate significant difference between groups (unpaired t-test, α = 0.05).

than the negatively charged MPA–AuNPs (Fig. 2(a)). PAH–AuNPs significantly affected daphnid mortality, eliciting 40% mortality at 10 μg L^{-1} ($U = 0$, $p < 0.05$).[13] MPA–AuNPs did not significantly affect daphnid survival at the highest concentration tested, 25 mg L^{-1} (data not shown) ($p > 0.05$).[13] The free ligands used in NP functionalization had no impact on daphnid survival at any concentration tested.

Daphnia magna chronic toxicity

Ligand–NP combination is also important in governing the chronic impacts on daphnid reproduction. Of the two NPs tested, PAH–AuNPs significantly decreased daphnid reproduction over the 21 day chronic exposure (Fig. 2(b)) while MPA–AuNPs did not (data not shown). PAH–AuNPs significantly decreased daphnid reproduction by 15% at the highest concentration tested, 5 μg L^{-1} ($F = 14.751$, df = 23, $p < 0.05$). In comparison, PAH free ligand caused a statistically insignificant increase in daphnid reproduction at 50 μg L^{-1}. As previously reported, 5 mg L^{-1} MPA free ligand increased daphnid reproduction by 14% ($U = 4$, $p < 0.05$, data not shown).[13]

Daphnia magna acute gene expression response

After a 24 h acute exposure, NP functionalization is also an important factor in determining *Daphnia* response at the

gene level when exposed to PAH and MPA–AuNPs, resulting in different gene expression patterns for *cat*, *nadh*, *vtg*, *gst* and *hsp70* (Fig. 2). For *Daphnia* exposed to PAH–AuNPs, there was a significant 0.74 fold decrease in the relative expression of *hsp70* (F = 31.799, df = 49, $P < 0.05$) compared to controls. *Daphnia* exposed to MPA–AuNPs caused a significant 1.36 fold increase for *hsp70* (F = 31.799, df = 49, $P < 0.05$), 1.49 fold increase for *nadh* (F = 29.066, df = 55, $p < 0.05$), 1.67 fold increase for *gst* (F = 23.116, df = 53, $p < 0.05$) and 3.12 fold increase for *vtg* (F = 11.556, df = 47, $p < 0.05$) over controls. MPA–AuNP-exposed *Daphnia* had significantly different gene expression patterns than *Daphnia* exposed to PAH–AuNPs for *nadh*, *vtg*, *gst* and *hsp70* (Fig. 2 and 5). Notably, PAH–AuNPs caused a 0.33 fold increase in relative expression of *vtg* while MPA–AuNPs elicited a 3.12 fold increase in relative expression of *vtg* (F = 11.556, df = 47, $p < 0.05$).

The impacts of free ligands used in particle functionalization closely follow the gene expression patterns observed for their respective functionalized NPs at 24 h (Fig. 2). *Daphnia* exposed to the PAH ligand showed no statistical difference compared to *Daphnia* exposed to PAH–AuNPs for all genes tested except *cat* (F = 8.640, df = 55, $p < 0.05$) and *vtg* (F = 11.556, df = 47, $p < 0.05$). Each gene that showed a significant positive fold change in relative expression for *Daphnia* exposed to MPA–AuNPs also showed a significant fold change in relative expression for the MPA free ligand treatment and did not significantly differ between the two.

Daphnia magna chronic gene expression response

Similar to the 24 h acute exposure, AuNP surface functionalization played an important role in determining gene expression levels in *Daphnia* chronically exposed to AuNPs (Fig. 2 and 5). For *Daphnia* exposed to PAH–AuNPs, there was a significant 1.33 fold decrease in the relative expression of *vtg* (F = 16.592, df = 42, $p < 0.05$) and a significant 0.87 fold increase in the relative expression of *act* (F = 9.68, df = 42, $p < 0.05$) over controls (Fig. 5). MPA–AuNPs elicited a significant 1.24, 0.82 and 0.93 fold decreases in the relative expression of *hsp70* (F = 9.294, df = 42, $p < 0.05$), *cat* (F = 18.128, df = 44, $p < 0.05$) and *nadh* (F = 14.9, df = 44, $p < 0.05$), respectively, compared to controls (Fig. 2 and 5). Notably, for this treatment, there was a significant 2.2 fold increase in the relative expression of *vtg* (F = 16.592, df = 42, $p < 0.05$) over controls (Fig. 2). A significantly different gene expression response was observed for several genes when AuNP treatments were compared. PAH–AuNP treatment elicited a positive fold change in the relative expression of *cat*, *nadh* and *act* while MPA–AuNP elicited a negative fold for these same genes. The greatest difference between these two treatments was observed for *vtg*.

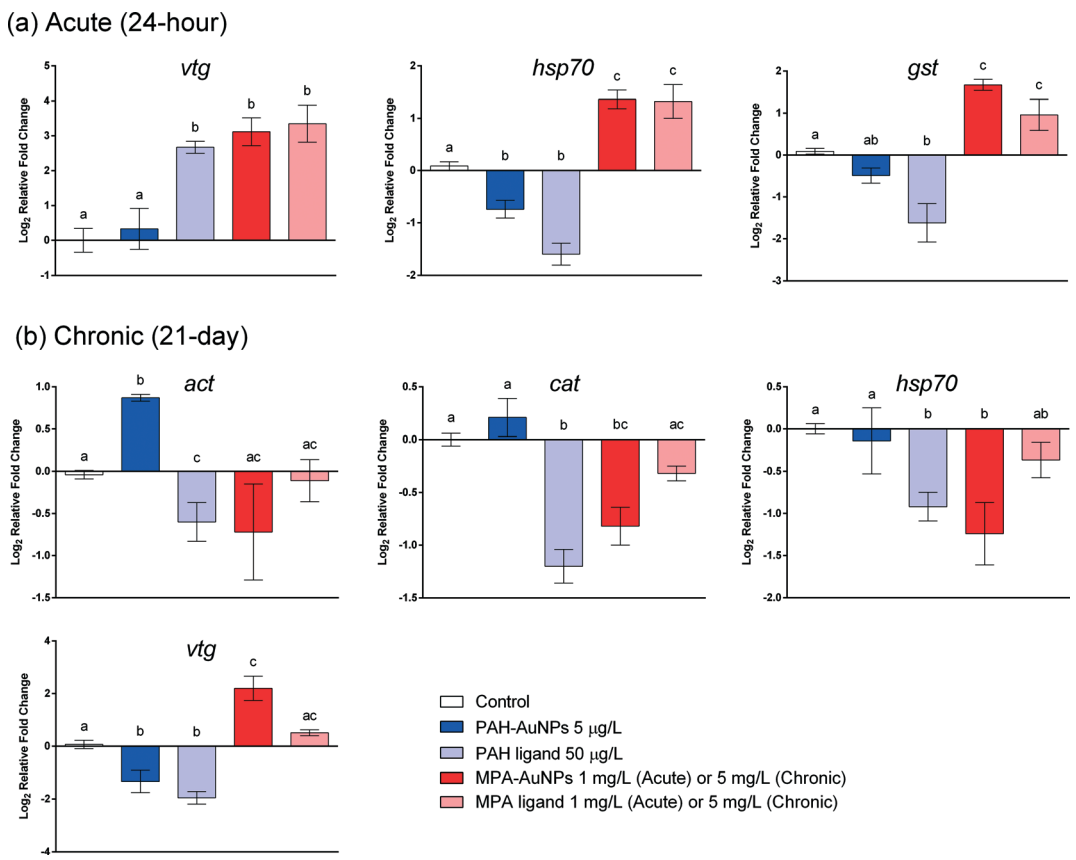

Fig. 5 Selected gene responses in *D. magna* upon AuNP/ligand exposure. Error bars show standard error of the mean ($n \geq 6$ for all exposure). All figures follow the same legend. Different letter designations between different groups indicate significant difference (Tukey's test, $\alpha = 0.05$).

NP-specific impacts were observed in *Daphnia* chronically exposed functionalized AuNPs *versus* their respective PAH and MPA ligands as reflected in the gene expression patterns (Fig. 2 and 5). PAH–AuNP and PAH ligand caused a similar relative expression pattern in *Daphnia* for genes *gst*, *hsp70*, *vtg* and *nadh*, as no significant difference was observed among these conditions (Fig. 2). However, PAH ligand caused 0.6 fold decrease in relative expression for *act* compared with the PAH–AuNP treatment that elicited a 0.98 fold increase in relative expression for *act* ($F = 9.68$, df = 42, $p < 0.05$) (Fig. 5). There were no significant differences between MPA ligand and MPA–AuNP treatments on *Daphnia* expression for any genes tested.

Discussion

Ligand–NP combinations differed in the extent of organismal apical endpoint impacts. Both model organisms were impacted to a greater extent by positively charged ligand–NP combinations with differential sensitivities. PAH–AuNPs were determined to be 2–3 orders of magnitude more toxic than the MPA–AuNPs for both *S. oneidensis* and *D. magna*. MPA–AuNPs caused no acute mortality in *D. magna* or inhibition on *S. oneidensis* oxygen uptake at the highest concentration tested (25 mg L^{-1} for daphnids and 5 mg L^{-1} for bacteria) (Fig. S2†).[13] PAH–AuNPs elicited mortality in *D. magna* at concentrations as low as 10 μg L^{-1} and decreases in reproduction at 5 μg L^{-1} (Fig. 1(a)),[13] while *S. oneidensis* started to show respiratory inhibition at 100 μg L^{-1} (Fig. 1(c)). Electrostatic interactions could largely drive the differences in sensitivity to the differently charged particles, as both eukaryotes and prokaryotes have cell surfaces that are negatively charged.[58,59] It is thought that, due to electrostatic interactions, positively charged NPs are more likely to interact with cell surfaces than negatively charged NPs. Goodman *et al.* (2004)[60] observed similar differences in the toxicity of AuNPs functionalized with cationic and anionic side chains when exposed to mammalian cell lines and bacterial cells, and Feng *et al.*[61] demonstrated a similar correlation between toxicity and NP-cell association where increased NP-cell association was found for positively charged NPs compared to negatively charged NPs in bacteria. In addition to electrostatic interactions, the low toxicity of MPA–AuNPs may be potentially explained by the high degree of aggregation of MPA–AuNPs experienced in both organisms' exposure media (Table 2), thus reducing bioavailability. Overall, similar differential toxicity of the two functionalized NPs were observed in our study in both model organisms, indicating these organisms may follow the same electrostatic mechanism for interacting with NPs despite having distinct membrane surface chemistry and that the general response of whole organism may be extrapolated from the response of cell lines, although they differ in sensitivity.

In some cases the toxicity of select NPs may not be determined by their respective ligand alone, which demonstrates NP-specific organismal impacts. However, this NP specific effect was only true for *D. magna*, where the impacts to *S. oneidensis* could largely be attributed to the ligand itself and only at much higher concentrations. The differences in sensitivity observed for these two model organisms exposed to PAH–AuNPs may be due to the distinct differences in the cell surface chemistry of Gram-negative bacteria and the aquatic eukaryotes. Besides the cytoplasmic membrane, which are found in both bacterial and *Daphnia* cells, the Gram-negative *S. oneidensis* bacterial cell also has an envelope that consists of a peptidoglycan–lipoprotein complex, periplasmic zone, and an outer membrane layer.[58] The outer membrane layer is the first barrier that NPs would encounter, and this lipid bilayer retains various amounts of embedded lipopolysaccharides (LPS).[58] LPS are high molecular weight molecules with a basal lipid anchored in the lipid bilayer and a long negatively charged chain of polysaccharide. Recent work using *S. oneidensis* demonstrated that LPS is an important binding site for AuNPs.[62] Compared to the animal cell membrane, the complex structure of the cell envelope in *S. oneidensis* may provide extra protection when NPs are in proximity to the cells, thus desensitizing bacterial cells to NP exposures. In addition, studies demonstrate that eukaryote cells have many more mechanisms for supramolecular and colloidal particle internalization (*e.g.* receptor mediated endocytosis, pinocytosis and phagocytosis) for both nano- and macro-sized particles, while very few studies show plausible evidence of internalization of nanomaterials into bacterial cells.[63–65] Furthermore, the manner by which multi- and single-cellular organisms interact with NPs may also contribute to the difference in sensitivity. *Daphnia* actively accumulate NPs internally while bacteria only passively interact with NPs through random encounters on the surface. The difference in how NP interact and accumulate in two organisms may also result in the NP-specific effect observed in *D. magna* but not in *S. oneidensis*. PAH–AuNPs resulted in a decrease in *Daphnia* survival (10 μg L^{-1}) while the respective PAH free ligand control (100 μg L^{-1}) did not show any mortality (Fig. 1(a)). However, when PAH–AuNPs elicited inhibition to bacterial oxygen uptake at 100 μg L^{-1}, the respective ligand control (1 mg L^{-1}) displayed a similar inhibition (Fig. 1(c)). These biological differences and impacts of NP surface functionalization and free ligand type are further addressed by the presented gene expression study.

Gene expression revealed insight into potentially molecular pathways that may be impacted upon exposure to NPs and may explain the differences in toxicity across different ligand–NP combinations and supported the mortality and respiration results indicating a particle- specific impact in *Daphnia versus Shewanella*. In both acute and chronic assays, *Daphnia* exposed to PAH–AuNPs elicited a significantly different gene expression pattern compared with *Daphnia* exposed to MPA–AuNPs, despite the two NPs having the same gold core. These differences were notable in the 24 h acute exposure for *hsp70*, *gst*, *vtg* and *nadh* and in the 21 day chronic assay for *hsp70*, *vtg*, *nadh*, *cat* and *act*. Amongst the genes

that responded, a positive relative fold change for *act* was unique to the PAH–AuNP treatment in the 21 day assay with respect to the ligand control. Actin (*act*) encodes for a protein important to cytoskeleton and muscle fibril production as well as other cell functions. Studies have linked an increase in protein concentration of actin as a compensatory mechanism to maintain muscular and cellular performance in times of environmental stress.[66] In addition, studies have indicated a high binding affinity of microparticles for actin[67] and have shown that multiple NP types damage actin filaments *in vitro*.[68–70] PAH–AuNPs could be potentially damaging muscle fibrils and cellular structure over long-term exposures in *Daphnia*. The relationship of this gene with apical endpoints impacted in *Daphnia* within this study remains unclear.

Daphnia exposed to MPA–AuNPs only uniquely responded to the treatment with an increase in the relative fold change of *gst* at 24 h. This gene encodes for an enzyme glutathione *S*-transferase and is an important enzyme in xenobiotic detoxification as it conjugates compounds with glutathione and may be elevated in times of oxidative stress. Our previous studies observed *gst* induction in *Daphnia* dependent upon NP functionalization of fullerenes but only at concentrations that elicited significant mortality (>5 mg L^{-1}).[9] Like MPA–AuNPs, these NPs exhibited a high degree of aggregation and exhibited low toxicity in *Daphnia*. This may demonstrate an acute whole organismal response to a high amount of negatively charged NPs. Our more recent previous study examined adult daphnid guts exposed to 4 nm PAH and MPA–AuNPs and their ligands at low concentrations (<0.05 mg L^{-1}).[18] Here, we showed that significant amounts of ROS were produced for both MPA and PAH AuNPs and their respective ligands at the same concentrations. This leads us to believe that ROS production does not fully explain the adverse outcomes observed in our acute and chronic studies. Therefore, other mechanisms may be responsible for the observed impacts as *Daphnia* responded differently to MPA and PAH AuNPs but had similar amounts of ROS detected upon exposure to these treatments at the same concentrations. However, in our current study and the previous, gene expression patterns were different for the two ligand–NP combinations. These results suggest that pathways affected by NPs are strongly dependent upon NP surface properties.

For *S. oneidensis*, gene expression assays were again indicative of the observed apical endpoint impacts. Most of the gene expression responses for *S. oneidensis* were provoked equally by the free ligand exposure and ligand–NP combination at both time points. While MPA–AuNPs did not show any impact that was specific to NPs, the decrease in expression of 16S at 6 hour exposure and *sodB* gene at 1 hour exposure were unique to the PAH–AuNPs but not to PAH free ligand. The *sodB* gene encodes for one of the superoxide dismutases (SODs) that protect cells from deleterious reactions with reactive oxygen species;[71] it has been previously reported that the *sodB* gene was up-regulated upon *S. oneidensis* exposure to chromium(VI).[72] More related, a previous study using 60 nm amino-functionalized polystyrene nanomaterial (PS-NH_2-NPs) on *E. coli* single-gene deletion mutants showed that the Δ*sodB* mutant was more sensitive to the exposure of PS-NH_2-NPs compared to the parent strain.[73] As PAH–AuNPs have a similar surface-functionalization of amine groups with PS-NH_2-NPs, these results suggests that the *sodB* gene plays an essential role in bacterial cell response to amine-functionalized nanomaterials, making it possible to use *sodB* as a biomarker for this specific NP surface functionalization. 16S ribosomal RNA (rRNA) is one of the three rRNAs, which are components of prokaryotic ribosomes. rRNA transcription is the rate-limiting step in ribosome synthesis, and thus, directly correlates to protein synthesis and cell growth.[74] Previous research has reported that rRNA degradation occurs during environmental stress, including oxidative stress and starvation.[75–77] Notably, it was also reported that rRNA is degraded due to a change in cell membrane permeability, potentially leading to the entry of RNase I, an endoribonuclease, from the periplasmic space into the cytoplasm.[78,79] Extensive cell membrane damage can also result in the efflux of RNA due to the loss of plasma membrane integrity.[80] Previous research has shown the disruption of membrane integrity in *S. oneidensis* cells upon PAH–AuNP exposure,[61] correlating with the decrease in the expression of 16S. It should be noted that at 1 hour exposure, the respective PAH ligand control also elicited decrease in 16S expression, while at 6 hour exposure only PAH–AuNPs showed the effect; thus, the potential of 16S to be used as a biomarker that is specific for PAH–AuNPs is limited to long-term exposures. In effort to link 16S and *sodB* gene response to the apical biological endpoints, the gene expression level of these two genes was examined at a higher dosage (100 μg L^{-1}) that also caused inhibition in bacterial oxygen uptake (Fig. 1(c)). While the *sodB* gene at 1 hour exposure did not elicit change in gene expression, 16S at 6 hour exposure showed a similar decrease upon 100 μg L^{-1} PAH–AuNP exposure (Fig. 4), proving that 16S can be potentially used as a biomarker for the impact of PAH–AuNPs on bacterial oxygen uptake; future work will explore the adverse outcome pathway from the decrease in 16S rRNA expression to the inhibition of bacterial oxygen uptake, and we postulate that the inhibition is mediated *via* reduced activity in protein synthesis. MPA–AuNPs did not induce a similar response of 16S rRNA expression, or any other NP-specific response, indicating a distinction between the same AuNP cores functionalized with different surface ligands.

Length of exposure had an impact on the effects seen in both species and on both gene expression and apical endpoints measured. Short-term exposures for both *D. magna* and *S. oneidensis* revealed that functionalized NP impacts on certain molecular pathways might be predicted by their respective ligand alone. Out of all *S. oneidensis* regulated genes, three genes stand out as potential predictors of NP impacts based on the ligand alone. These genes are *pspB* and *rpoA* for PAH–AuNP/ligand and *ibpA* for MPA–AuNP/ligand at 1 hour exposure, as they were influenced similarly upon

exposure to both the ligand-bound AuNPs and the respective free ligand. For *D. magna*, three genes were most notable; these genes were *hsp70 and vtg* for PAH–AuNP/ligand and *hsp70*, *vtg* and *nadh* for MPA–AuNP/ligand. These results suggest that NP impacts on specific molecular pathways may be predicted based on response to the ligand alone. This finding is especially important for ligands or functional groups that are commonly used to achieve desired physiochemical properties for NPs. However, as demonstrated with our study, ligand–NP combinations did alter several genes that the ligand alone did not, and the concentrations of NPs that impacted apical endpoints, in particular PAH–AuNPs, differed from that of the ligand. This diminishes the potential ability to use ligand information alone as a predictor for NP toxicity; rather, the overall NP characteristics, including charge or size, may be more informative.

Our study revealed that gene expression in acute exposures was not predictive of long-term impacts or differences among treatments with respect to ligand *versus* ligand–NP combinations. In addition, long-term exposure to NPs resulted in gene expression patterns that could not be predicted based on gene expression patterns from short-term exposures. Upon exposure to MPA–AuNP/ligand, both *S. oneidensis* and *D. magna* showed decreases in gene expression during short-term exposure and that this response flipped to mostly an increase in gene expression upon long-term exposure. Exceptions to this finding were observed in the decrease of 16S and *sodB* expression upon PAH–AuNP exposure in S. *oneidensis* and the increase of *vtg* gene expression upon MPA–AuNP exposure in *D. magna*, which show similar response in gene expression levels at both time points. Our results indicate that, although it is possible to predict long-term gene expression impacts based on short-term impacts, it is limited to selected genes, which may downplay the significance of this finding.

Gene expression responses across organisms provide an indication of how organisms are similar or different in their response to NP exposures. A notable signature shared across two organisms was the up-regulation of *ibpA*/*hsp70* induced by MPA–AuNP and ligand for short-term exposures. Both *ibpA* and *hsp70* encode for heat shock protein in *S. oneidensis* and *D. magna*, respectively. Heat shock proteins (Hsp) are a large family of proteins that help unfolded or misfolded proteins to fold correctly *in vivo* and are widely considered to be good indicators of proteotoxic stress.[81,82] The up-regulation of heat shock protein induced by MPA–AuNPs and ligands potentially indicates the disruption of membrane proteins, provoking pathways that help adapt to change in chemical environment caused by introduction of NPs or ligands. This feature, shared by both organisms, potentially indicates a universal stress-response to negatively charged NPs, making the genes encoding for heat shock protein a good candidate for predicting the effect of NPs based on the response to their respective ligands. However, MPA–AuNPs did not lead to any adverse outcomes at the concentrations we tested, which makes understanding the importance of this pathway within the context of our study difficult.

Conclusion

Molecular studies have the ability to tease out distinct modes of action for NP toxicity and help to develop biomarkers for assessing NP impacts on environmentally relevant endpoints. Using standard toxicological and gene expression assays, we revealed that: 1) the ligand–NP combinations determine the extent of impacts on apical endpoints and the toxicity of select NPs may not be determined by their respective ligand alone; 2) depending on the organism considered, exposure to ligand–NP combinations may impact unique molecular pathways that differ from the ligand alone; 3) short-term exposures reveal that ligand–NP impacts on certain molecular pathways might be predicted by their respective ligand alone but the ability to predict long-term impacts may be minimal; and 4) examining gene expression responses across organisms may provide an indication of how organisms are similar or different in their response to NP exposures. Lastly, this study reveals that there are mechanisms other than oxidative stress for NP toxicity and that these may be elucidated using molecular level experiments and exposures that consider sub-lethal concentrations.

Acknowledgements

This work was funded by the National Science Foundation Center for Chemical Innovations grant CHE-1240151: Center for Sustainable Nanotechnology and a Research Experience for Undergraduates fellowship supported by the National Science Foundation Center for Chemical Innovation Program (CHE-1240151) awarded to Ky G. Christenson. We thank Ky G. Christenson for his help in gene expression work. We wish to thank the UWM Great Lakes Genomics Center for the use of equipment and assistance by staff. Lastly, we want to thank Dr. Y. Hayashi for access to the NORMA-Gene workbook.

References

1 A. S. Arico, P. Bruce, B. Scrosati, J.-M. Tarascon and W. van Schalkwijk, *Nat. Mater.*, 2005, **4**, 366–377.
2 J. Xie, G. Liu, H. S. Eden, H. Ai and X. Chen, *Acc. Chem. Res.*, 2011, **44**, 883–892.
3 M. M. Pendergast and E. M. V. Hoek, *Energy Environ. Sci.*, 2011, **4**, 1946–1971.
4 A. Nel, T. Xia, L. Madler and N. Li, *Science*, 2006, **311**, 622–627.
5 Y. Pan, S. Neuss, A. Leifert, M. Fischler, F. Wen, U. Simon, G. Schmid, W. Brandau and W. Jahnen-Dechent, *Small*, 2007, **3**, 1941–1949.
6 A. Albanese, P. S. Tang and W. C. Chan, *Annu. Rev. Biomed. Eng.*, 2012, **14**, 1–16.
7 D. A. Arndt, M. Moua, J. Chen and R. D. Klaper, *Environ. Sci. Technol.*, 2013, **47**, 9444–9452.

8 R. Klaper, D. Arndt, K. Setyowati, J. Chen and F. Goetz, *Aquat. Toxicol.*, 2010, **100**, 211–217.
9 R. Klaper, J. Crago, J. Barr, D. Arndt, K. Setyowati and J. Chen, *Environ. Pollut.*, 2009, **157**, 1152–1156.
10 B. D. Chithrani, A. A. Ghazani and W. C. Chan, *Nano Lett.*, 2006, **6**, 662–668.
11 H. Yang, C. Liu, D. Yang, H. Zhang and Z. Xi, *J. Appl. Toxicol.*, 2009, **29**, 69–78.
12 K. L. Aillon, Y. Xie, N. El-Gendy, C. J. Berkland and M. L. Forrest, *Adv. Drug Delivery Rev.*, 2009, **61**, 457–466.
13 J. S. Bozich, S. E. Lohse, M. D. Torelli, C. J. Murphy, R. J. Hamers and R. D. Klaper, *Environ. Sci.: Nano*, 2014, **1**, 260–270.
14 A. M. El Badawy, R. G. Silva, B. Morris, K. G. Scheckel, M. T. Suidan and T. M. Tolaymat, *Environ. Sci. Technol.*, 2010, **45**, 283–287.
15 C. He, Y. Hu, L. Yin, C. Tang and C. Yin, *Biomaterials*, 2010, **31**, 3657–3666.
16 N. M. Schaeublin, L. K. Braydich-Stolle, A. M. Schrand, J. M. Miller, J. Hutchison, J. J. Schlager and S. M. Hussain, *Nanoscale*, 2011, **3**, 410–420.
17 A. Verma and F. Stellacci, *Small*, 2010, **6**, 12–21.
18 G. A. Dominguez, S. E. Lohse, M. D. Torelli, C. J. Murphy, R. J. Hamers, G. Orr and R. D. Klaper, *Aquat. Toxicol.*, 2015, **162**, 1–9.
19 A. Albanese and W. C. W. Chan, *ACS Nano*, 2011, **5**, 5478–5489.
20 N. Lewinski, V. Colvin and R. Drezek, *Small*, 2008, **4**, 26–49.
21 N. Khlebtsov and L. Dykman, *Chem. Soc. Rev.*, 2011, **40**, 1647–1671.
22 C.-W. Lam, J. T. James, R. McCluskey, S. Arepalli and R. L. Hunter, *Crit. Rev. Toxicol.*, 2006, **36**, 189–217.
23 E. Fröhlich, *Int. J. Nanomed.*, 2012, **7**, 5577–5591.
24 S. K. Sohaebuddin, P. T. Thevenot, D. Baker, J. W. Eaton and L. Tang, *Part. Fibre Toxicol.*, 2010, **7**, 22.
25 M. Heinlaan, A. Ivask, I. Blinova, H.-C. Dubourguier and A. Kahru, *Chemosphere*, 2008, **71**, 1308–1316.
26 H. Sanderson and M. Thomsen, *Bull. Environ. Contam. Toxicol.*, 2007, **79**, 331–335.
27 D. R. Moore, R. L. Breton and D. B. MacDonald, *Environ. Toxicol. Chem.*, 2003, **22**, 1799–1809.
28 A. A. Shvedova, A. Pietroiusti, B. Fadeel and V. E. Kagan, *Toxicol. Appl. Pharmacol.*, 2012, **261**, 121–133.
29 B. J. Marquis, S. A. Love, K. L. Braun and C. L. Haynes, *Analyst*, 2009, **134**, 425–439.
30 A. Manke, L. Wang and Y. Rojanasakul, *BioMed Res. Int.*, 2013, **2013**, 942916.
31 E. J. Park and K. Park, *Toxicol. Lett.*, 2009, **184**, 18–25.
32 R. Klaper, D. Arndt, J. Bozich and G. Dominguez, *Analyst*, 2014, **139**, 882–895.
33 F. Gottschalk, T. Sonderer, R. W. Scholz and B. Nowack, *Environ. Sci. Technol.*, 2009, **43**, 9216–9222.
34 A. Valavanidis, T. Vlahogianni, M. Dassenakis and M. Scoullos, *Ecotoxicol. Environ. Saf.*, 2006, **64**, 178–189.
35 R. Franco, R. Sanchez-Olea, E. M. Reyes-Reyes and M. I. Panayiotidis, *Mutat. Res., Genet. Toxicol. Environ. Mutagen.*, 2009, **674**, 3–22.
36 T. Finkel and N. J. Holbrook, *Nature*, 2000, **408**, 239–247.
37 J. Ryan and L. Hightower, *Stress-Inducible Cellular Responses*, Springer, 1996, pp. 411–424.
38 C. G. Kilty, J. Keenan and M. Shaw, *Expert Opin. Drug Saf.*, 2007, **6**(2), 207–215.
39 C. Eason and K. O'Halloran, *Toxicology*, 2002, **181**, 517–521.
40 N. J. Niemuth, R. Jordan, J. Crago, C. Blanksma, R. Johnson and R. D. Klaper, *Environ. Toxicol. Chem.*, 2014, **34**(2), 291–296.
41 G. T. Ankley, K. M. Jensen, M. D. Kahl, J. J. Korte and E. A. Makynen, *Environ. Toxicol. Chem.*, 2001, **20**, 1276–1290.
42 S. M. Johns, M. D. Kane, N. D. Denslow, K. H. Watanabe, E. F. Orlando, D. L. Villeneuve, G. T. Ankley and M. S. Sepúlveda, *Environ. Toxicol. Chem.*, 2009, **28**, 873–880.
43 J. S. Garvey, *Preprints of Papers Presented at National Meeting, Division of Water, Air and Waste Chemistry*, American Chemical Society, (USA), 1988.
44 M. Fischbach, E. Sabbioni and P. Bromley, *Cell Biol. Toxicol.*, 1993, **9**, 177–188.
45 H. H. Hau and J. A. Gralnick, *Annu. Rev. Microbiol.*, 2007, **61**, 237–258.
46 R. Gulati, *Hydrobiologia*, 1978, **59**, 101–112.
47 N. R. Jana, L. Gearheart and C. J. Murphy, *Langmuir*, 2001, **17**, 6782–6786.
48 T. K. Sau and C. J. Murphy, *J. Am. Chem. Soc.*, 2004, **126**, 8648–8649.
49 D. A. Giljohann, D. S. Seferos, W. L. Daniel, M. D. Massich, P. C. Patel and C. A. Mirkin, *Angew. Chem., Int. Ed.*, 2010, **49**, 3280–3294.
50 S. F. Sweeney, G. H. Woehrle and J. E. Hutchison, *J. Am. Chem. Soc.*, 2006, **128**, 3190–3197.
51 J. A. Yang, S. E. Lohse and C. J. Murphy, *Small*, 2014, **10**, 1642–1651.
52 C. J. Ackerson, P. D. Jadzinsky and R. D. Kornberg, *J. Am. Chem. Soc.*, 2005, **127**, 6550–6551.
53 M. D. Torelli, R. A. Putans, Y. Tan, S. E. Lohse, C. J. Murphy and R. J. Hamers, *ACS Appl. Mater. Interfaces*, 2015, **7**, 1720–1725.
54 EPA, *Standard operating procedure for moderately hard reconstituted water*, SoBran, Dayton, OH, USA, 2003.
55 S. Zhao and R. D. Fernald, *J. Comput. Biol.*, 2005, **12**, 1047–1064.
56 L.-H. Heckmann, P. Sorensen, P. Krogh and J. Sorensen, *BMC Bioinf.*, 2011, **12**, 250.
57 S. Wang, W. Lu, O. Tovmachenko, U. S. Rai, H. Yu and P. C. Ray, *Chem. Phys. Lett.*, 2008, **463**, 145–149.
58 P. A. Rice and B. H. Iglewski, *Rev. Infect. Dis.*, 1988, **10**, S277–S278.
59 A. Martínez-Palomo, *International Review of Cytology*, Academic Press, 1970, vol. 29, pp. 29–75.
60 C. M. Goodman, C. D. McCusker, T. Yilmaz and V. M. Rotello, *Bioconjugate Chem.*, 2004, **15**, 897–900.
61 Z. V. Feng, I. L. Gunsolus, T. A. Qiu, K. R. Hurley, L. H. Nyberg, H. Frew, K. P. Johnson, A. M. Vartanian, L. M. Jacob, S. E. Lohse, M. D. Torelli, R. J. Hamers, C. J. Murphy and C. L. Haynes, *Chem. Sci.*, 2015, DOI: 10.1039/C5SC00792E.
62 K. H. Jacobson, I. L. Gunsolus, T. R. Kuech, J. M. Troiano, E. S. Melby, S. E. Lohse, D. Hu, W. B. Chrisler, C. J. Murphy,

G. Orr, F. M. Geiger, C. L. Haynes and J. A. Pedersen, *Environ. Sci. Technol.*, 2015, DOI: 10.1021/acs.est.5b01841.
63 Y. Y. Zhao, Y. Tian, Y. Cui, W. W. Liu, W. S. Ma and X. Y. Jiang, *J. Am. Chem. Soc.*, 2010, **132**, 12349–12356.
64 S. Dalai, S. Pakrashi, R. S. Kumar, N. Chandrasekaran and A. Mukherjee, *Toxicol. Res.*, 2012, **1**, 116–130.
65 A. Kumar, A. K. Pandey, S. S. Singh, R. Shanker and A. Dhawan, *Chemosphere*, 2011, **83**, 1124–1132.
66 S. Schwerin, B. Zeis, T. Lamkemeyer, R. J. Paul, M. Koch, J. Madlung, C. Fladerer and R. Pirow, *BMC Physiol.*, 2009, **9**, 8.
67 M. Ehrenberg and J. L. McGrath, *Acta Biomater.*, 2005, **1**, 305–315.
68 P. Ruenraroengsak and A. T. Florence, *J. Drug Targeting*, 2010, **18**, 803–811.
69 V. G. Walker, Z. Li, T. Hulderman, D. Schwegler-Berry, M. L. Kashon and P. P. Simeonova, *Toxicol. Appl. Pharmacol.*, 2009, **236**, 319–328.
70 T. Mironava, M. Hadjiargyrou, M. Simon, V. Jurukovski and M. H. Rafailovich, *Nanotoxicology*, 2010, **4**, 120–137.
71 S. B. Farr and T. Kogoma, *Microbiol. Rev.*, 1991, **55**, 561–585.
72 K. Chourey, M. R. Thompson, J. Morrell-Falvey, N. C. VerBerkmoes, S. D. Brown, M. Shah, J. Zhou, M. Doktycz, R. L. Hettich and D. K. Thompson, *Appl. Environ. Microbiol.*, 2006, **72**, 6331–6344.
73 A. Ivask, E. Suarez, T. Patel, D. Boren, Z. Ji, P. Holden, D. Telesca, R. Damoiseaux, K. A. Bradley and H. Godwin, *Environ. Sci. Technol.*, 2012, **46**, 2398–2405.
74 B. J. Paul, W. Ross, T. Gaal and R. L. Gourse, *Annu. Rev. Genet.*, 2004, **38**, 749–770.
75 D. R. Crawford, Y. H. Wang, G. P. Schools, J. Kochheiser and K. J. A. Davies, *Free Radical Biol. Med.*, 1997, **22**, 551–559.
76 G. N. Basturea, M. A. Zundel and M. P. Deutscher, *RNA*, 2011, **17**, 338–345.
77 D. Hsu, L.-M. Shih and Y. C. Zee, *J. Bacteriol.*, 1994, **176**, 4761–4765.
78 M. P. Deutscher, *Nucleic Acids Res.*, 2006, **34**, 659–666.
79 M. Kuwano, H. Taniguchi, M. Ono, H. Endo and Y. Ohnishi, *Biochem. Biophys. Res. Commun.*, 1977, **75**, 156–162.
80 Z. Darzynkiewicz, S. Bruno, G. Delbino, W. Gorczyca, M. A. Hotz, P. Lassota and F. Traganos, *Cytometry*, 1992, **13**, 795–808.
81 S. D. Brown, M. R. Thompson, N. C. VerBerkmoes, K. Chourey, M. Shah, J. Z. Zhou, R. L. Hettich and D. K. Thompson, *Mol. Cell. Proteomics*, 2006, **5**, 1054–1071.
82 K. Chourey, M. R. Thompson, J. Morrell-Falvey, N. C. VerBerkmoes, S. D. Brown, M. Shah, J. Z. Zhou, M. Doktycz, R. L. Hettich and D. K. Thompson, *Appl. Environ. Microbiol.*, 2006, **72**, 6331–6344.